Author/s:
Dadu, RHR;Ford, R;Sambasivam, P;Gupta, D

Title:
Evidence of early defence to Ascochyta lentis within the recently identified Lens orientalis resistance source ILWL180

Date:
2018-09-01

Citation:
Dadu, R. H. R., Ford, R., Sambasivam, P. & Gupta, D. (2018). Evidence of early defence to Ascochyta lentis within the recently identified Lens orientalis resistance source ILWL180. Plant Pathology, 67 (7), pp.1492-1501. https://doi.org/10.1111/ppa.12851.

Persistent Link:
https://hdl.handle.net/11343/283811

MR. RAMA HARINATH REDDY DADU (Orcid ID : 0000-0002-9699-4518)

DR. DORIN GUPTA (Orcid ID : 0000-0003-2375-0237)

Article type : Original Article

Running head recto: Early defence to Ascochyta lentis

Running head verso: R. H. R. Dadu et al.

Evidence of early defence to *Ascochyta lentis* within the recently identified *Lens orientalis* resistance source ILWL180

R. H. R. Dadu[a], R. Ford[b], P. Sambasivam[bc] and D. Gupta[a]*

[a]*School of Agriculture and Food, The University of Melbourne, Dookie Campus, VIC;* [b]*Environmental Futures Research Institute, School of Natural Sciences, Griffith University, Nathan Campus, QLD; and* [c]*Faculty of Veterinary and Agricultural Sciences, The University of Melbourne, Parkville Campus, VIC, Australia*

*E-mail: dorin.gupta@unimelb.edu.au

In plant–pathogen interactions, strong structural and biochemical barriers may induce a cascade of reactions *in planta*, leading to host resistance. The kinetic speed and amplitudes of these defence mechanisms may discriminate resistance from susceptibility to necrotrophic fungi. The infection processes of two *Ascochyta lentis* isolates (FT13037 and F13082) on the recently identified ascochyta blight (AB)-resistant *Lens orientalis* genotype ILWL180 and two cultivated genotypes, ILL7537 (resistant) and ILL6002 (susceptible), were assessed. Using histopathological methods, significant differences in early behaviour of the isolates and the subsequent differential defence responses of the hosts were revealed. Irrespective of virulence, both isolates had significantly lower germination, shorter germ tubes and delayed

appressorium formation on the resistant genotypes (ILWL180 and ILL7537) compared to the susceptible genotype (ILL6002); furthermore, these were more pronounced on genotype ILWL180 than on genotype ILL7537. Subsequently, host perception of pathogen entry led to the faster accumulation and notably higher amounts of reactive oxygen species and phenolic compounds at the penetration sites of the resistance genotypes ILWL180 and ILL7537. In contrast, genotype ILL6002 responded slowly to the *A. lentis* infection and reaffirmed previous gross disease symptomology reports as highly susceptible. Interestingly, quantification of H_2O_2 was markedly higher in ILWL180 particularly at 12 hpi compared to ILL7537, potentially indicative of its superior resistance capability. Faster recognition of *A. lentis* is likely to be a major contribution to the superior resistance observed in genotype ILWL180 to the highly aggressive isolates of *A. lentis* assessed.

Keywords: Ascochyta lentis, histopathology, *Lens orientalis,* lentil, phenolic compounds, reactive oxygen species

Introduction

Ascochyta blight (AB) of lentil, caused by *Ascochyta lentis*, is the most widespread fungal disease across lentil cultivating regions globally (Ye *et al.*, 2003). Seedling infection can destroy an entire crop, whilst infection at podding/maturity results in poor seed quality (Gossen & Morrall, 1983) and substantial yield losses (Brouwer *et al.*, 1995). In Australia alone, the epidemics of AB have caused an estimated A$15.3 million of losses to the lentil industry (Murray & Brennan, 2012). Although fungicides are mostly effective, improving lentil resistance is vital to manage the disease more sustainably.

Significant numbers of resistance sources have been identified and deployed in resistance breeding programmes around the world (Ali, 1995; Erskine *et al.*, 1996; Nasir & Bretag, 1998; Vandenberg *et al.*, 2000). However, continuous reliance on relatively few resistance sources in Australia and Canada that also contain desirable agronomic and yield characteristics has probably led to erosion of resistance genes in elite cultivars (Laird, Northfield and Nipper) through selection of more aggressive isolates (Ahmed & Morrall, 1996; Nasir & Bretag, 1997; Davidson *et al.*, 2016). Therefore, there is an urgent need to identify and introgress novel AB resistance genes/alleles to enhance the longevity of defence mechanisms within elite Australian cultivars. For this, wild species of lentil have been

identified as potential reservoirs of useful resistance genes/alleles (Tullu *et al.*, 2010; Dadu *et al.*, 2017) and interspecific fertile hybrids were successfully produced using conventional techniques (Gupta & Sharma, 2007; Tullu *et al.*, 2013). To aid in this, an understanding of the key defence responses within target resistant wild accessions is necessary.

Ascochyta lentis is a necrotrophic fungus and uses an appressorium-based penetration peg to penetrate the external cuticular layers before colonizing the host tissue. Successful invasion and colonization ultimately leads to disease symptoms of necrotic lesions speckled with pseudothecia containing pycnidiospores (Roundhill *et al.*, 1995). During the process of infection, conidia of *A. lentis* germinate within 2 h post-inoculation (hpi) and develop a bulb-like appressorium at the tip of the germ tube in the following 6–8 h leading to penetration of the host cell (Roundhill *et al.*, 1995). This then induces a series of defence mechanisms in plants that include physiological, biochemical and molecular responses.

Roundhill *et al.* (1995) suggested a mere contact of pathogen on the leaf surface is sufficient to regulate the first line of defences in lentil. The initial response of the infected cell following tissue penetration is an aggregation of cytoplasm and development of papillae, which interrupts further spread of the pathogenic hyphae (Roundhill *et al.*, 1995). Later, microarray profiling of resistant (ILL7537) and susceptible (ILL6002) lentil lines revealed the first transcriptional responses of lentil to *A. lentis* (Mustafa *et al.*, 2009). The results showed that most of the differential expression (DE) in resistant ILL7537 took place within 6–48 hpi, whereas in susceptible ILL6002 this extended up to 96 hpi. The short period of transcriptional regulation in ILL7537 compared to ILL6002 may indicate rapid recognition of *A. lentis* infection and early expression of defence proteins. The DE profile of both genotypes included genes related to biochemical and structural defences such as the expression of reactive oxygen species (ROS), synthesis of pathogenesis-related (PR) proteins and lignification. However, the delayed activation of defence responses, particularly after 72 and 96 hpi, in ILL6002, may have led to susceptibility (Mustafa *et al.*, 2009).

Consequently, the up-regulation of these genes within ILL7537 may have caused reduction in percentage conidial germination, germ tube length and percentage appressoria formation, thereby restricting disease development (Sambasivam *et al.*, 2016). In addition to the physical reasons for delayed fungal establishment in ILL7537, these histopathological studies also reported the accumulation of ROS, cell wall thickening and cytoplasmic aggregation as part of biochemical and structural defence responses in ILL7537 (Sambasivam

et al., 2016). Conversely, the absence of these events in ILL6002 may have been responsible for the observed susceptibility. Also, ROS are well known to trigger a cascade of defence responses such as cell wall strengthening, transcription of defence-related genes and hypersensitive cell death that subsequently restrict pathogen growth (Hückelhoven & Kogel, 2003; Lin *et al.*, 2005).

The most recent study on the lentil–*A. lentis* interaction, with a single aggressive isolate (AL4) from Australia, observed defence-related differential gene expression using RNA sequencing within 2 hpi (Khorramdelazad *et al.*, 2018). Several genes that are representative of key defence functions, such as fungal elicitor recognition and early signalling (2 hpi), structural response (6 hpi), biochemical response (6 hpi), hypersensitive reaction and cell death (24 hpi), and systemic acquired resistance (24 hpi) were revealed. Several of these responses validated the previous findings of Mustafa *et al.* (2009) and provided the genetic components potentially underpinning the defence-related histopathological observations by Sambasivam *et al.* (2016). In general, the resistant ILL7537 was able to initiate key defence-related genetic responses faster and at higher amplitudes than the susceptible ILL6002. However, efficacy of this timing may be largely dependent on the host genotype involved. Therefore, there is a need to fully understand the diversity in timing of previously well-characterized defence responses prior to establishing it as a reliable resistance source.

Thus, the aim of this study was to assess the physiological and biochemical defence responses employed by ILWL180, a lentil line with reportedly higher resistance than ILL7537, in response to *A. lentis* infection. Also, the timings of these responses were characterized in comparison to the previously assessed resistant ILL7537 and the susceptible ILL6002 to determine whether *Lens orientalis* ILWL180 resistance is discriminant.

Materials and methods

Plant material

Lens orientalis ILWL180 was procured from the Australian Grains Genebank, Horsham, Victoria. Two *Lens culinaris* genotypes, ILL7537 (resistant control) and ILL6002 (susceptible control), were supplied by the Faculty of Veterinary and Agriculture Sciences

(FVAS), Dookie Campus, The University of Melbourne. Three seeds of each genotype replicated four times (four pots) were sown in 10 cm diameter pots filled with pine bark soil, fertilized with Nitrosol, Amsgrow (4.5 mL L^{-1}) weekly and watered on alternate days. Prior to sowing, seeds of ILWL180 were soaked in water overnight to enhance germination and were also sown 7 days earlier than the control genotypes to ensure all seedlings were at the same stage of maturity at inoculation on 14 and 21 days after sowing (DAS) for controls and wild genotype, respectively. After sowing, pots were placed in a Conviron growth cabinet at Dookie campus, The University of Melbourne and maintained at 18 ± 1 °C, 12 h/12 h day/night photoperiod with 300 μmol m^{-2} s^{-1} of light.

Fungal material

Single spore cultures of one aggressive isolate (FT13037) and one nonaggressive isolate (F13082) were supplied by the South Australian Research and Development Institute (SARDI), South Australia. Aggressiveness of isolate FT13037 was previously identified by Dadu *et al.* (2017) and isolate F13082 was identified as nonaggressive on a set of host differentials in a controlled bioassay (Davidson, SARDI, Adelaide, personal communication). Spore suspensions were prepared from 14-day-old fungal cultures as described previously (Dadu *et al.*, 2017).

Experimental design for evaluating fungal structures

Spore germination, germ tube length and appressorium formation of isolates (FT13037 and F13082) were assessed to evaluate the infection process at 6, 12, 20 and 30 hpi in all three genotypes using detached and attached leaf assays. Experiments were conducted in a completely randomized design with four replicates sown for each time point per isolate and one leaflet from each replicate was used to assess the development of the infection structures. A total of 100 spores (25 spores per corner of each leaflet) per replication were examined to calculate spore germination and appressorium percentage, and 100 random germinated spores from each replicate were observed to measure germ tube length. Image processing and analysis was carried out in IMAGEJ v. 1.50i software (Java) to measure germ tube length. Criteria for determining spore germination, germ tube length and appressoria formation were as described by Sambasivam *et al.* (2016).

Evaluation of infection process by detached leaf assay

Fully expanded 21-day-old leaflets from ILWL180, and 14-day-old leaflets from ILL7537 and ILL6002 were detached separately for each isolate and time point. Immediately after excision, for each time point, one leaflet from each of four replicates of each host/isolate interaction was sterilized, inoculated and incubated as described by Sambasivam *et al.* (2016). After 6, 12, 20 or 30 hpi leaflets were fixed and cleared to remove chlorophyll by immersing them in ethanol:glacial acetic acid (1:2 v/v) for 36 h with at least one change of clearing solution at 24 h (Sambasivam *et al.*, 2016). Cleared leaflets were stained with lactophenol cotton blue (Sigma Aldrich) for 5 min and visualized for fungal structures using a BHC light microscope (Olympus). Images were captured using a digital sight DS-Fi2 camera (Nikon).

Evaluation of infection process by attached/intact leaf assay

In the attached leaf assay, pots of all genotypes were inoculated using an air-pressurized hand-held sprayer at a concentration of 2×10^6 spores mL^{-1}. To enable uniform spread of inoculum droplets on the abaxial side of leaflets, pots were tilted slightly at a 45° angle and then sprayed with a fine mist of inoculum until run-off. Soon after inoculation, plants were covered with paper cups coated with wax (In Hospitality) and arranged randomly before carefully placing them in the growth cabinet under dark conditions at 16–18 °C and 98% relative humidity (RH). One leaflet from each of four replicates of each host × isolate interaction was selected and detached carefully at each time point. Subsequently, the detached leaflets were fixed, cleared and stained as described above to visualize fungal structures.

Experimental design for biochemical analysis of ROS and phenolic compounds

Histochemical localization of ROS (O_2^- and H_2O_2) and phenolic compounds were assessed at 12, 24 and 48 hpi in the detached leaflets of all three genotypes. Experiments were conducted in a completely randomized design and one leaflet each (two leaflets each for

quantifying H_2O_2) was assessed from the four replications at each time point to detect the responses to isolates FT13037 and F13082.

Histochemical localization of hydrogen peroxide (H_2O_2)

H_2O_2 release in detached leaflets of lentil was examined using a modified 3,3-diaminobenzidine (DAB) staining method as described by Thordal-Christensen *et al.* (1997). Detached leaflets of all three genotypes were inoculated as described above and incubated for 12, 24 and 48 h, after which leaflets were immediately immersed in 1 mg mL^{-1} HCl-acidified DAB (pH 3.8) solution and incubated in the dark at room temperature for 8 h. As described above, leaflets were fixed, cleared and stained before detecting accumulation of H_2O_2 as reddish-brown colouration at the sites of hyphal penetration and neighbouring cells using a BHC light microscope. The images were captured using a digital sight DS-Fi2 camera.

Quantification of H_2O_2

H_2O_2 produced in response to *A. lentis* infection was quantified using a modified ferrous xylenol orange (FOX) assay (Bellincampi *et al.*, 2000). Briefly, point-inoculated detached leaflets of the three genotypes, each weighing a minimum of 50 mg, were each homogenized in 10 mL 10 mM phosphate buffer (pH 7.0) using a mortar and pestle. Subsequently, the homogenate was filtered through a 250 mm sieve and centrifuged at 5488 ***g*** for 13 min. The resultant supernatant (1.5 mL) was then added to an equal volume of assay reagent (500 µM ammonium ferrous sulphate, 50 mM H_2SO_4, 200 µM xylenol orange and 200 mM sorbitol). Subsequently, the assay mixture was incubated for 45 min and absorbance of the FOX complex was measured at 560 nm using a Novaspec II spectrophotometer. To determine the amount of H_2O_2 in the leaflets, standard solutions of different concentrations of H_2O_2 ranging from 5 to 80 µM were prepared in distilled water. An aliquot of 1.5 mL of each concentration was added with an equal volume of assay reagent and incubated for 45 min. The absorbance of the FOX complex was measured at 560 nm and a standard calibration curve was plotted between concentrations of H_2O_2 and absorbance A_{560} to estimate the amount of H_2O_2 from the resultant regression equation. The concentration of H_2O_2 was expressed as µM per g fresh weight (FW).

Histochemical localization of superoxide anion (O_2^-)

O_2^- production by lentil in response to *A. lentis* infection was determined using a nitroblue tetrazolium (NBT) staining method as described by Ge *et al.* (2013). Leaflets from all three genotypes were detached, inoculated and incubated as described above. At 12, 24 and 48 hpi, leaflets were vacuum infiltrated in 50 mM sodium phosphate buffer (pH 7.5) containing 0.2% NBT for 1 h at room temperature. The leaflets were then fixed, cleared and stained as described above. Subsequently, the leaflets were examined for superoxide release using a BHC light microscope fitted with a digital sight DS-Fi2 camera. Dark blue deposits at the hyphal penetration sites and neighbouring cells indicated O_2^- release.

Histochemical localization of phenolic compounds

To detect phenolic compound deposition, inoculated leaflets were cleared at 12, 24 and 48 hpi using ethanol:glacial acetic acid (1:2 v/v) as described above. Cleared leaflets were stained using 0.05% toluidine blue in 0.1 M phosphate buffer (pH 5.5) for 1 h and examined under a BHC light microscope for greenish-blue deposits corresponding to phenolic compound accumulation (Ge *et al.*, 2013). The images were captured using a digital sight DS-Fi2 camera.

Statistical analysis

Percentage germination data were square root-transformed prior to statistical analysis and graphs were prepared with original back-transformed percentage data. Significant differences for square root-transformed percentage germination, germ tube length, percentage appressorium formation, and H_2O_2 quantification were identified via analysis of variance (ANOVA) tests within GENSTAT 16th edition software. Localization of ROS and phenolic compounds were observed as either present or absent.

Results

Infection process and physiological differences

Spore germination

In both assays and at all time points, significant differences among the three genotypes were observed for percentage spore germination of isolates FT13037 and F13082 ($P < 0.01$). Independent of whether the leaf was detached or not, both isolates germinated within 6 hpi on all three genotypes. However, the rate of germination on all three genotypes differed for both isolates and gradually increased between 6 hpi and 30 hpi ($P < 0.01$). At 30 hpi, a mean of 75.86% and 69.37% spores of isolates FT13037 and F13082, respectively, had germinated on the detached leaflets of the three genotypes (Fig. 1). In contrast, only 25.77% of FT13037 and 19.69% of F13082 spores had germinated when the leaflets were attached to the plants when inoculated. Further, among the three genotypes, the lowest spore germination for the aggressive isolate FT13037 at 30 hpi was observed for ILWL180, with a mean of 70.77% and 15.49% on detached and attached leaflets, respectively.

Germ tube length

Significantly shorter mean germ tube lengths were recorded for the nonaggressive isolate F13082 compared to the aggressive isolate FT13037 on all three genotypes in both the detached and attached assays ($P < 0.01$). Interestingly, germ tubes of both isolates were significantly shorter when inoculated on leaflets attached to plants compared to detached leaflets ($P < 0.01$). However, slightly longer germ tubes were observed on intact leaflets of ILWL180 for isolate FT13037 at 20 and 30 hpi. Significant differences between the isolates were detected on all three genotypes irrespective of time point ($P < 0.01$), although, the shortest germ tubes for both isolates were produced on ILWL180 (Fig. 2).

Appressoria

On detached leaflets, by 6 hpi, spores of the aggressive isolate FT13037 produced appressoria on genotypes ILL6002 and ILL7537. The percentage of germinating spores that had produced appressoria increased gradually to reach 27.13% and 9.8% on ILL6002 and ILL7537 respectively, by 30 hpi. In contrast, no appressoria were produced until 12 hpi on ILWL180, with a maximum mean of 8.79% by 30 hpi. Meanwhile, spores of the nonaggressive isolate F13082 did not produce appressoria until 12 hpi on ILWL180 and ILL7537, and just 2.69% produced appressoria on ILL6002 at 6 hpi. A significant difference in this trait was observed for isolate F13082 among all three genotypes and at 12, 20 and 30

hpi. At 30 hpi, the most appressoria were observed on ILL6002 (11.68%) and the least on ILWL180 (7.57%; $P < 0.01$; Fig. 3a).

On intact leaflets, unlike on detached leaflets, spores of the aggressive isolate FT13037 did not produce appressoria until 20 hpi on ILWL180 and ILL7537 and until 12 hpi on ILL6002 (Fig. 3b). Spores of the nonaggressive isolate F13082 did not produce appressoria until 30 hpi on ILWL180 and ILL7537 and until 12 hpi on ILL6002. Significant differences among frequencies of appressoria formation were recorded for both isolates among the three genotypes ($P < 0.01$). At 30 hpi, the highest and lowest percentage of appressoria formation by isolate FT13037 was observed on ILL6002 (10.46%) and ILWL180 (3.82%), respectively. Similarly, at 30 hpi with isolate F13082, the highest (5.11%) and lowest (1.47%) percentage of appressoria formation was observed on attached leaflets of ILL6002 and ILWL180, respectively.

Biochemical analysis of ROS

Localization of H_2O_2

The release of H_2O_2 in infected lentil leaflets of all three genotypes coincided with the formation of appressoria and was detected underneath the appressoria (Figs 4 & 5). However, visible differences in the intensity of H_2O_2 production were detected between the three genotypes (Figs 4 & 5). Accumulation of H_2O_2 gradually increased in the cells surrounding the infected region over time in the two resistant genotypes, ILWL180 and ILWL 7537 (Figs 4a–c & 5a–c). This response was weaker and restricted directly to the infected cells in the susceptible genotype ILL6002 (Figs 4d & 5d).

Quantification of H_2O_2

The concentration of H_2O_2 in the leaflets of all three genotypes was determined using a standard curve produced from known concentrations of H_2O_2 at A_{560} ($R^2 = 0.9857$; Fig. 6). The trends of production over time were then determined in all three genotypes in response to the aggressive and nonaggressive isolates (Figs 7 & 8).

The production of H_2O_2 in all three lentil genotypes was detected as early as 12 hpi (Figs 7 & 8) in response to *A. lentis* infection. Although the trend of H_2O_2 accumulation was similar among the three genotypes, concentrations among them were significantly different

($P < 0.01$) at each time point (Figs 7 & 8). ILWL180 responded quickly to the infection and subsequently produced higher concentrations of H_2O_2 ranging from 43.92 to 73.12 µM per g FW within 24 hpi; in contrast, by 24 hpi, the resistant control ILL7537 had lower concentrations, ranging from 5.85 to 65.82 µM per g FW. Leaflets of the susceptible genotype ILL6002 contained negligible concentrations of H_2O_2 at 12 hpi, with a maximum of only 57.42 µM per g FW H_2O_2 at 24 hpi.

Localization of O_2^-

Similar to the release of H_2O_2, O_2^- production also coincided with the formation of appressoria for both isolates on the three genotypes and was detected underneath the appressoria as early as 12 hpi (Fig. 4e). However, the response was delayed on ILWL180 until 24 hpi for isolate F13082 (Fig. 5e), which was probably caused by the delayed formation of appressoria, as reported above. A gradual and sustained increase in the accumulation of O_2^- at the infection sites was observed in the resistant genotypes ILWL180 and ILL7537 (Figs 4e–g & 5e–g), which did not occur in the susceptible genotype ILL6002 (Figs 4h & 5h).

Localization of phenolic compounds

Visible differences were observed among the three genotypes for production of phenolic compounds and their localization (Figs 4i–l & 5i–l). Much like H_2O_2 and O_2^- production, accumulation of phenolic compounds was detected beneath the appressoria and lining the cell walls of infected cells. Visible differences were apparent in the intensity and timing of accumulation. In the resistant genotypes, ILWL180 and ILL7537, accumulation of phenolic compounds was detected as early as 12 hpi and by 24 hpi in response to isolate FT13037 and isolate F13082, respectively, before gradually increasing at 48 hpi (Figs 4i–k & 5i–k). In contrast, phenolic compounds were not detected in the susceptible genotype ILL6002 until 24 hpi for both isolates. Following inoculation with isolate FT13037, the amount of phenolic compounds surrounding the infected region increased at 48 hpi (Fig. 4l). This was not observed for isolate F13082 (Fig. 5l).

Discussion

Upon recognition of necrotrophic fungal pathogens, plants display strong and complex defence responses that deter pathogen entry. In lentil, several structural, biochemical and molecular responses were previously reported to underpin defence to *A. lentis* (Roundhill *et al.*, 1995; Mustafa *et al.*, 2009; Sambasivam *et al.*, 2016). In the present study, physiological and biochemical defence responses to *A. lentis* were evaluated to determine the early defence mechanisms within the *L. orientalis* resistance source ILWL180.

Previous histopathology assays employed detached leaf tissues for evaluating plant–pathogen interactions (Armstrong-Cho *et al.*, 2012; Sambasivam *et al.*, 2016) and the conclusions were subsequently applied to whole plants. In contrast, attached leaflets were assessed along with detached leaflets in the present work and the comparison of results showed significant differences between the two assays. For all three host genotypes, when challenged with each of the two fungal isolates detached leaflets displayed higher conidial germination, longer germ tubes and higher percentages of appressorial formation than attached leaflets. Similarly, differences were detected between detached and attached leaf assays for length of primary hyphae produced by *Colletotrichum lentis* on lentil (Armstrong-Cho *et al.*, 2012). The detachment process may affect systemic hormone defence-related signalling and probably initiates senescence in the leaflets, contributing to the faster invasion of the pathogen (Liu *et al.*, 2007). *Ascochyta lentis* infected detached leaflets much earlier than intact leaflets due to the compromised defence responses, regardless of resistance status of the genotypes. These observed differences in resistance to AB between detached and intact leaflets could be further validated either through the use of defence-impaired mutants or by gene expression studies. By doing so, it would be possible to detect which defence responses are affected by detachment of the leaflets. Previously, detachment was reported to compromise the salicylic acid- and jasmonate/ethylene-dependent signalling pathways of *Arabidopsis thaliana*, leading to easier penetration and aggressive colonization by *Colletotrichum linicola* A1 and *Colletotrichum higginsianum* (Liu *et al.*, 2007). Furthermore, these compromised defence responses may potentially bridge the knowledge gap regarding the genes that are involved in the early defence responses and thereby may assist the efforts to identify and develop AB resistant varieties through marker-assisted selection (MAS).

As with previous reports, prepenetration events were genotype-specific (Sambasivam *et al.*, 2016; Sari *et al.*, 2017), with both isolates exhibiting differential germination percentages, germ tube lengths, as well as timing and percentage of appressoria formation on both the attached and detached leaflets of the three genotypes assessed. These results provide

further evidence of the presence of different defence mechanisms among lentil genotypes. In the present work, and as previously reported (Sambasivam *et al.*, 2016; Sari *et al.*, 2017), conidial germination of both isolates was significantly higher on the attached leaflets of the susceptible genotype ILL6002 than on the resistant genotype ILL7537. However, lowest percentages of conidial germination were observed on the leaflets of ILWL180 for both isolates. This may be due to the early recognition of the pathogen through pathogen-activated molecular patterns (PAMPs) and pattern recognition receptors (PRRs) including receptor-like kinase proteins and receptor-like proteins (Dangl *et al.*, 2013). In previous reports of the ILL7537–*A. lentis* interaction, protein kinases such as leucine-rich repeat receptor kinase (LRR-RK) and calmodulin domain protein kinase (CDPK) were found to play key roles in early signalling of downstream defence responses (Khorramdelazad, *et al.*, 2018). In addition, the dense hairy nature of ILWL180 leaflets might also have led to a reduction of germination by obstructing the deposition of spores on the leaf surface, as similarly observed in Masoor-93, a resistant cultivar from Pakistan (Sahi *et al.*, 2000).

Successfully germinated conidia of *A. lentis* develop germ tubes that help penetration into host tissues by producing an appressorium at their tip (Roundhill *et al.*, 1995). In previous reports, longer germ tubes and higher appressoria frequencies were determined as indicators of host susceptibility to *A. lentis* (Sambasivam *et al.*, 2016; Sari *et al.*, 2017). Similarly, in the present work, conidia of both isolates produced longer germ tubes and higher appressorial percentages on the detached and intact leaflets of the susceptible genotype ILL6002 compared to those of the resistant ILL7537 and ILWL180. Furthermore, shorter germ tubes and lower appressoria frequencies were detected on ILWL180 compared to ILL7537, as also reported on another *Lens ervoides* accession L-01-827A (Sari *et al.*, 2017). This is probably due to the timing of activation of structural and biochemical defence responses. Structural defence responses include papillae formation at the point of penetration to entrap the penetration peg (Roundhill *et al.*, 1995). Sambasivam *et al.* (2016) demonstrated the earlier formation of papillae in resistant genotype ILL7537 compared to genotype ILL6002. Accordingly, differentially elevated transcript levels of laccase diphenol oxidase (PPOl) and exocyst subunit 70A1 family protein (Exo70A1), linked to papillae formation, were detected as early as 2 hpi in ILL7537, much earlier than in ILL6002 (Khorramdelazad *et al.*, 2018).

Host biochemical defences include production of antifungal compounds, such as proteinaceous inhibitors and pathogenesis-related proteins (PR), to counteract the penetration

of tissue by the pathogen. Proteinaceous inhibitors such as pectin methylesterase inhibitor (PMEI), auxin-repressed protein (ARP) and polygalacturonase inhibitor (PGIP), involved in countering cell wall-degrading enzymes (CWDE) released by fungi, were found to be significantly over-expressed in ILL7537 compared to ILL6002 (Khorramdelazad *et al.*, 2018). Similarly, elevated levels of PR proteins PR2 and PR4, known for cell lysis and limiting the growth of fungi, respectively, were more highly expressed in ILL7537 and 964A-46 than ILL6002 (Mustafa *et al.*, 2009; Vaghefi *et al.*, 2013). Based on the different defence mechanisms of different genotypes shown above, ILWL180 may have different genes with more efficient molecular defence mechanism to counter *A. lentis* infection compared to that of ILL7537.

Together with the differences observed in percentage of appressoria formed among the three genotypes, significant differences were also evident in time taken for the conidia of both isolates to develop the first appressorium. On ILL6002, the first appressorium was formed at 6 or 12 hpi on the detached or attached leaflets, respectively. However, this was delayed until 12 and 20 hpi on the detached and attached leaflets, respectively, on ILWL180. Similarly, Sambasivam *et al.* (2016) found differences in time taken for appressorium formation on the detached leaflets of three genotypes with known resistances.

Following early recognition of the pathogen and consequent signal transduction, plants activate a battery of defence mechanisms. Among them, an oxidative burst with rapid generation of ROS such as O_2^- and H_2O_2 is considered as one of the earliest defence response (Doke, 1983). In the current study, all three genotypes produced H_2O_2 and O_2^- in response to appressorium penetration by both isolates at 12, 24 and 48 hpi. However, significant differences in magnitude of H_2O_2 and O_2^- production occurred between the genotypes up to 24 hpi, with concentrations in ILWL180 being greater than in ILL7537 and even lower in ILL6002. Later, quantification of H_2O_2 revealed a decrease in H_2O_2 at 48 hpi in all three genotypes with the aggressive isolate FT13037 but only in the resistant genotypes with the nonaggressive FT13082. Overall, H_2O_2 production in ILWL180 was significantly higher at all time points than in ILL7537 (particularly at 12 hpi). This provides further evidence that early release and accumulation of ROS is a major mechanism employed by resistant lentil to limit the growth of *A. lentis in planta* (Sambasivam *et al.*, 2016).

This is the first histological report to capture O_2^- involvement in the defence response of lentil to *A. lentis*. However, this is an intermediate response, because O_2^- is rapidly

converted to H_2O_2 by superoxide dismutase (SOD), as previously shown to be elevated during the interaction (Mustafa *et al.*, 2009). This helps to explain why the elevated levels of H_2O_2 were detected more in the infected and neighbouring cells compared to O_2^-, which was confined to the penetration sites on all genotypes. Apart from direct toxicity to the invading pathogen, the diffusible nature of ROS, particularly H_2O_2, across cell membranes leads to signalling of downstream defence mechanisms including cell wall strengthening (Lin *et al.*, 2005) and synthesis of PR proteins (Hancock *et al.*, 2007), which together lead to the expression of the hypersensitive reaction (Lam, 2004). In addition, elicitation of ROS also induces the activation of phenylpropanoid metabolism in plants (Jabs *et al.*, 1997) to synthesize phenolic compounds (Dalkin *et al.*, 1990). Accordingly, comparatively higher ROS production in resistant genotypes such as ILWL180 and ILL7537 probably increases accumulation of phenolic compounds in the infected and surrounding cells, leading to deposition of lignin for physical strengthening, and synthesis of antimicrobial compounds such as phytoalexins at the infection site.

In conclusion, based on the physical and biochemical evidence presented, it is proposed that the *L. orientalis* genotype ILWL180 is a superior and potentially useful source of resistance to *A. lentis.* This is achieved through delayed prepenetration events and relatively faster and stronger accumulation of ROS and phenolic compounds to limit the growth and spread of *A. lentis* post-penetration. Future investigations involving differential molecular studies of the specific biological steps within the defence mechanism will be helpful to elucidate the potential novelty of ILWL180. Additionally, analysis of segregation populations developed among the known resistant genotypes including ILWL180 may decipher the allelic relationships among them and whether the resistance genes are novel.

Acknowledgements

The authors wish to thank The University of Melbourne and the Victorian Government for the Victoria–India Doctoral Scholarship (VIDS) and Melbourne International Fee Remission Scholarship (MIFRS) to R.H.R.D. to support this work at The University of Melbourne. The authors would also like to thank Richard W. S. Nicholas Trust for funding this work. There are no conflicts of interest among authors about this paper.

References

Ahmed S, Morrall RAA, 1996. Field reactions of lentil lines and cultivars to isolates of *Ascochyta fabae* f. sp. *lentis*. *Canadian Journal of Plant Pathology* **18**, 362–9.

Armstrong-Cho C, Wang J, Wei Y, Banniza S, 2012. The infection process of two pathogenic races of *Colletotrichum truncatum* on lentil, *Canadian Journal of Plant Pathology* **34**, 58–67.

Bellincampi D, Dipierro N, Salvi G, Cervone F, De Lorenzo G, 2000. Extracellular H_2O_2 induced by oligogalacturonides is not involved in the inhibition of the auxin-regulated *rolB* gene expression in tobacco leaf explants. *Journal of Plant Physiology* **122**, 1379–86.

Brouwer JB, Bretag TW, Materne MA, 1995. Coordinated improvement program for Australian lentils. In: *Proceedings of the 2nd European Conference on Grain Legumes, Copenhagen, Denmark*. Washington DC, USA: Association of Educational Publishers, 25.

Dadu RHR, Ford R, Sambasivam P, Gupta D, 2017. A novel *Lens orientalis* resistance source to the recently evolved highly aggressive Australian *Ascochyta lentis* isolates. *Frontiers in Plant Science* **8**, 1038.

Dalkin K, Edwards R, Edington B, Dixon RA, 1990. Stress responses in alfalfa (*Medicago sativa* L.) I. Induction of phenylpropanoid biosynthesis and hydrolytic enzymes in elicitor-treated cell suspension cultures. *Plant Physiology* **92**, 440–6.

Dangl JL, Horvath DM, Staskawicz BJ, 2013. Pivoting the plant immune system from dissection to deployment. *Science* **341**, 746–51.

Davidson J, Smetham G, Russ MH *et al.*, 2016. Changes in aggressiveness of the *Ascochyta lentis* population in southern Australia. *Frontiers in Plant Science* **7**, 393.

Doke N, 1983. Involvement of superoxide anion generation in the hypersensitive response of potato tuber tissues to infection with an incompatible race of *Phytophthora infestans* and to the hyphal wall components. *Physiological Plant Pathology* **23**, 345–57.

Erskine W, Bayaa B, Saxena, MC, 1996. Registration of ILL 5588 lentil germplasm resistant

to vascular wilt and AB. *Crop Science* **36**, 1080.

Ge Y, Bi Y, Guest DI, 2013. Defence responses in leaves of resistant and susceptible melon (*Cucumis melo* L.) cultivars infected with *Colletotrichum lagenarium*. *Physiological and Molecular Plant Pathology* **81**, 13–21.

Gossen BD, Morrall RAA, 1983. Effect of ascochyta blight on seed yield and quality of lentils. *Canadian Journal of Plant Pathology* **5**, 168–73.

Gupta D, Sharma SK, 2007. Widening the gene pool of cultivated lentils through introgression of alien chromatin from wild *Lens* subspecies. *Plant Breeding* **126**, 58–61.

Hancock J, Desikan R, Harrison J, Bright J, Hooley R, Neill S, 2007. Doing the unexpected: proteins involved in hydrogen peroxide perception. *Journal of Experimental Botany* **57**, 1711–8.

Hückelhoven R, Kogel KH, 2003. Reactive oxygen intermediates in plant–microbe interactions: who is who in powdery mildew resistance? *Planta* **216**, 891–902.

Jabs T, Tschfpe M, Colling C, Hahlbrock K, Scheel D, 1997. Elicitor-stimulated ion fluxes and O_2^- from the oxidative burst are essential components in triggering defense gene activation and phytoalexin synthesis in parsley. *Proceedings of the National Academy of Sciences of the United States of America* **94**, 4800–5.

Khorramdelazad M, Bar I, Whatmore P *et al.*, 2018. Transcriptome profiling of lentil (*Lens culinaris*) through the first 24 hours of *Ascochyta lentis* infection reveals key defence response genes. *BMC Genomics* **19**, 108.

Lam E, 2004. Controlled cell death, plant survival and development. *Nature Reviews Molecular Cell Biology* **5**, 305–15.

Lin W, Hu X, Zhang W Rogers WJ, Cai W, 2005. Hydrogen peroxide mediates defense responses induced by chitosans of different molecular weights in rice. *Journal of Plant Physiology* **162**, 937–44.

Liu G, Kennedy R, Greenshields DL *et al.*, 2007. Detached and attached *Arabidopsis* leaf assays reveal distinctive defense responses against hemibiotrophic *Colletotrichum* spp.

Molecular Plant–Microbe Interactions **20**, 1308–19.

Murray GM, Brennan JP, 2012. *The Current and Potential Costs from Diseases of Pulse Crops in Australia*. Canberra, Australia: Grains Research and Development Cooperation.

Mustafa BM, Coram TE, Pang ECK, Taylor PWJ, Ford R, 2009. A cDNA microarray approach to decipher AB resistance in lentil. *Australasian Plant Pathology* **38**, 617–31.

Nasir M, Bretag TW, 1997. Pathogenic variability in Australian isolates of *Ascochyta lentis*. *Australasian Plant Pathology* **26**, 217–20.

Nasir M, Bretag, TW, 1998. Reactions of lentil accessions from 25 different countries to Australian isolates of *Ascochyta lentis*. *Genetic Resources and Crop Evolution* **45**, 297–9.

Roundhill SA, Fineran BA, Cole ALJ, Ingerfeld M, 1995. Structural aspects AB of lentil. *Canadian Journal of Botany* **73**, 485–97.

Sahi ST, Randhawa MA, Khan SM, 2000. Morphological basis of resistance in lentil (*Lens culínarís* Medik.) against ascochyta blight. *Pakistan Journal of Biological Sciences* **3**, 1277–80.

Sambasivam P, Taylor PWJ, Ford R, 2016. Pathogenic variation and virulence related responses of *Ascochyta lentis* on lentil. *European Journal of Plant Pathology* **147**, 265.

Sari E, Bhadauria V, Vandenberg A, Banniza S, 2017. Genotype-dependent interaction of lentil lines with *Ascochyta lentis*. *Frontiers in Plant Science* **8**, 764.

Thordal-Christensen H, Zhang Z, Wei YD, Collinge DB, 1997. Subcellular localization of H_2O_2 in plants. H_2O_2 accumulation in papillae and hypersensitive response during the barley-powdery mildew interaction. *The Plant Journal* **11**, 1187e94.

Tullu A, Banniza S, Tar'an B, Warkentin T, Vandenberg A, 2010. Sources of resistance to ascochyta blight in wild species of lentil (*Lens culinaris* Medik.). *Genetic Resources and Crop Evolution* **57**, 1053–63.

Tullu A, Bett K, Banniza S, Vail S, Vandenberg A, 2013. Widening the genetic base of cultivated lentil through hybridization of *Lens culinaris* 'Eston' and *L. ervoides* accession IG 72815. *Canadian Journal of Plant Pathology* **93**, 1037–47.

Vaghefi N, Mustafa BM, Dulal N, Selby-Pham J, Taylor PWJ, Ford R, 2013. A novel pathogenesis-related protein (LcPR4a) from lentil, and its involvement in defence against *Ascochyta lentis*. *Phytopathologia Mediterranea* **52**, 192–201.

Vandenberg A, Kiehn FA, Vera C *et al.*, 2000. CDC Milestone lentil. *Canadian Journal of Plant Science* **81**, 113–4.

Ye G, McNeil DL, Hill GD, 2003. Breeding for resistance to lentil AB. *Plant Breeding* **121**, 185–91.

Figure legends

Figure 1 Percentage spore germination of *Ascochyta lentis* isolates FT13037 and F13082 at 6, 12, 20 and 30 h post-inoculation (hpi) on three lentil genotypes ILWL180, ILL6002 and ILL7537 in (a) detached leaflet assay and (b) intact leaflet assay.

Figure 2 Germ tube length of *Ascochyta lentis* isolates FT13037 and F13082 at 6, 12, 20 and 30 h post-inoculation (hpi) on three lentil genotypes ILWL180, ILL6002 and ILL7537 in (a) detached leaflet assay and (b) intact leaflet assay.

Figure 3 Percentage formation of appressoria of *Ascochyta lentis* isolates FT13037 and F13082 at 6, 12, 20 and 30 h post-inoculation (hpi) on three lentil genotypes ILWL180, ILL6002 and ILL7537 in (a) detached leaflet assay and (b) intact leaflet assay.

Figure 4 Histochemical localization of biochemical defence responses elicited within the leaflets of lentil genotypes ILWL180, ILL7537 and ILL6002 in response to *Ascochyta lentis* isolate FT13037. (a–d) Detection of hydrogen peroxide (H_2O_2) production by 3,3-diaminobenzidine (DAB) staining method. Arrowheads indicate accumulation of reddish-brown deposits beneath the appressoria and surrounding cells. (e–h) Accumulation of superoxide (O_2^-) stained using the nitroblue tetrazolium method. Dark blue deposits beneath the appressoria represent O_2^- production (arrowheads). (i–l) Accumulation of phenolic compounds, detected by staining with toluidine blue. Arrowheads indicate greenish-blue

deposits due to accumulation of phenolic compounds within the infected and surrounding cells. Scale bars represent 50 µm (a, b, c, e, f, i & l) and100 µm (d, g, h, j & k).

Figure 5 Histochemical localization of biochemical defence responses elicited within the leaflets of lentil genotypes ILWL180, ILL7537 and ILL6002 in response to *Ascochyta lentis* isolate F13082. (a–d) Detection of hydrogen peroxide (H_2O_2) production by 3,3-diaminobenzidine (DAB) staining method. Arrowheads indicate accumulation of reddish-brown deposits beneath the appressoria and surrounding cells. (e–h) Accumulation of superoxide (O_2^-) stained using the nitroblue tetrazolium method. Dark blue deposits beneath the appressoria represent O_2^- production (arrowheads). (i–l) Accumulation of phenolic compounds detected by staining with toluidine blue. Arrowheads indicate greenish-blue deposits due to accumulation of phenolic compounds within the infected and surrounding cells. Scale bars represent 50 µm (a, b, c, e, f, g, i, k & l) and 100 µm (d, h & j).

Figure 6 Standard calibration curve of absorbance at 560 nm versus concentration of hydrogen peroxide (H_2O_2; µM).

Figure 7 Concentration of hydrogen peroxide (H_2O_2) produced in lentil genotypes ILWL180, ILL7537 and ILL6002 in response to the aggressive *Ascochyta lentis* isolate FT13037 at 12, 24 and 48 h post-inoculation (hpi).

Figure 8 Concentration of hydrogen peroxide (H_2O_2) produced in lentil genotypes ILWL180, ILL7537 and ILL6002 in response to the nonaggressive *Ascochyta lentis* isolate F13082 at 12, 24 and 48 h post-inoculation (hpi).

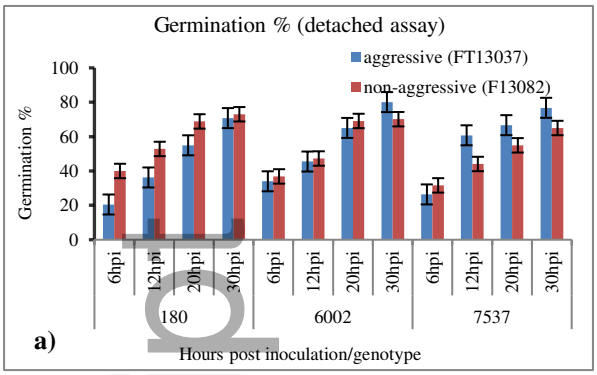

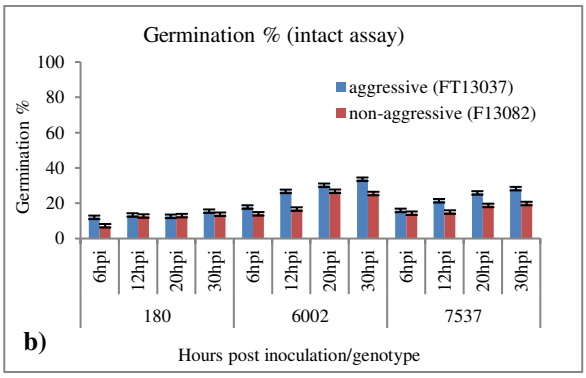

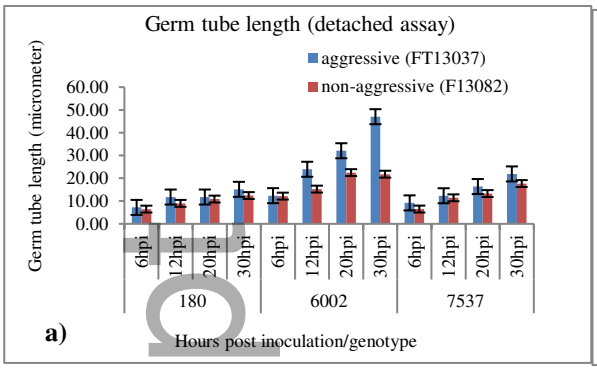

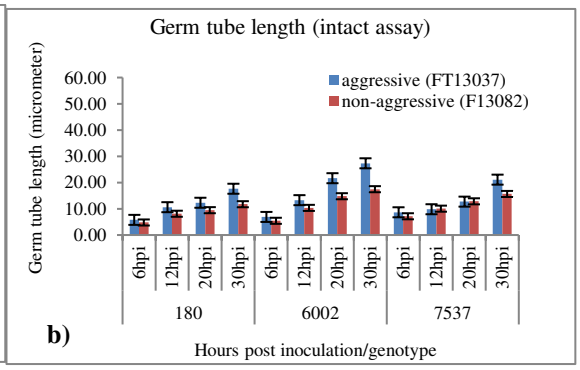

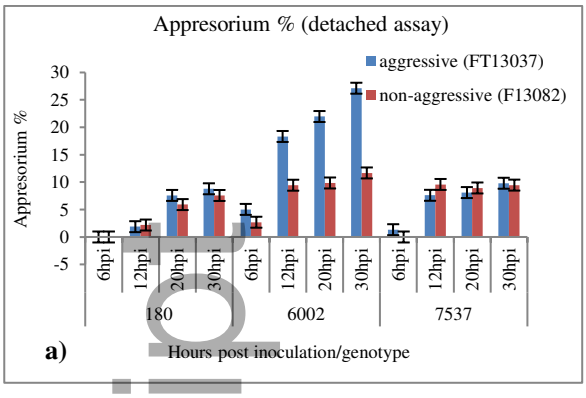

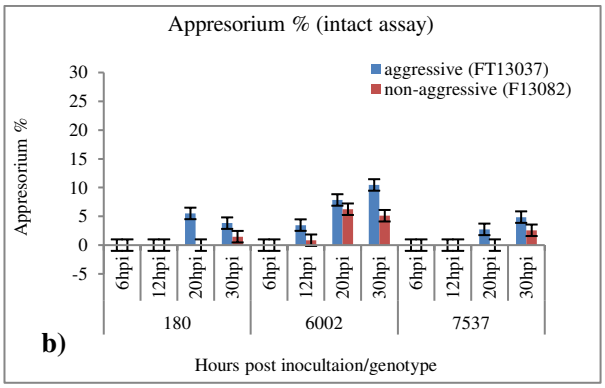

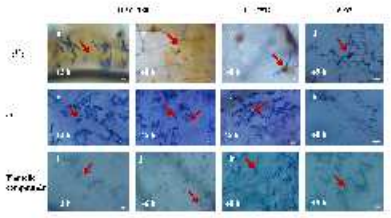

ppa_12851_f4_aa.tif

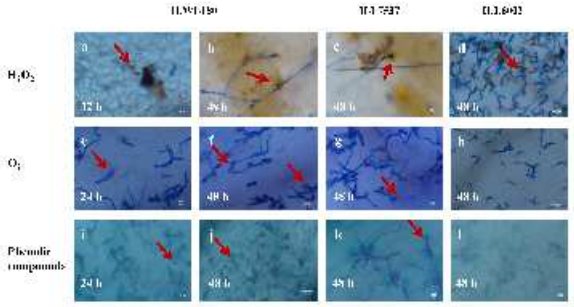

ppa_12851_f5_aa.tif

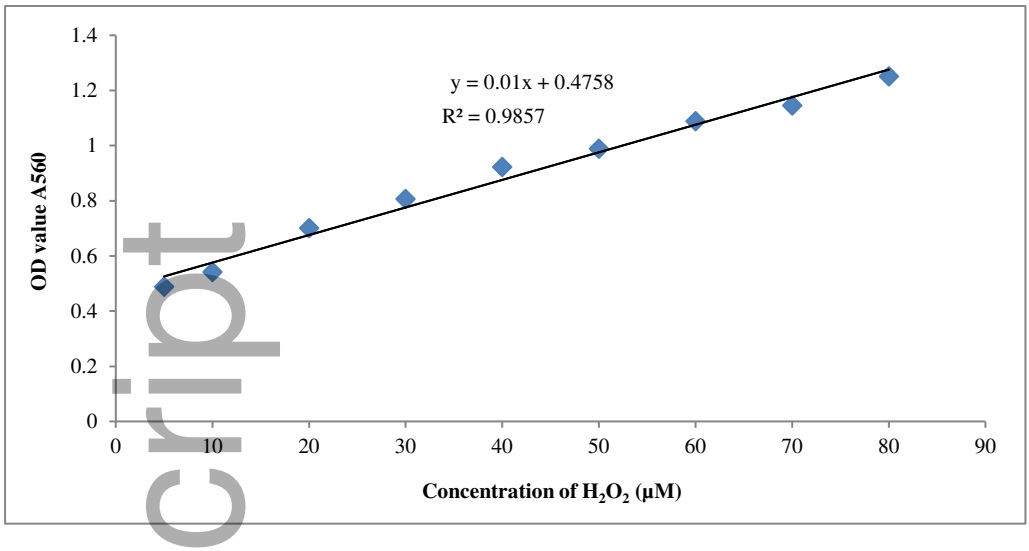

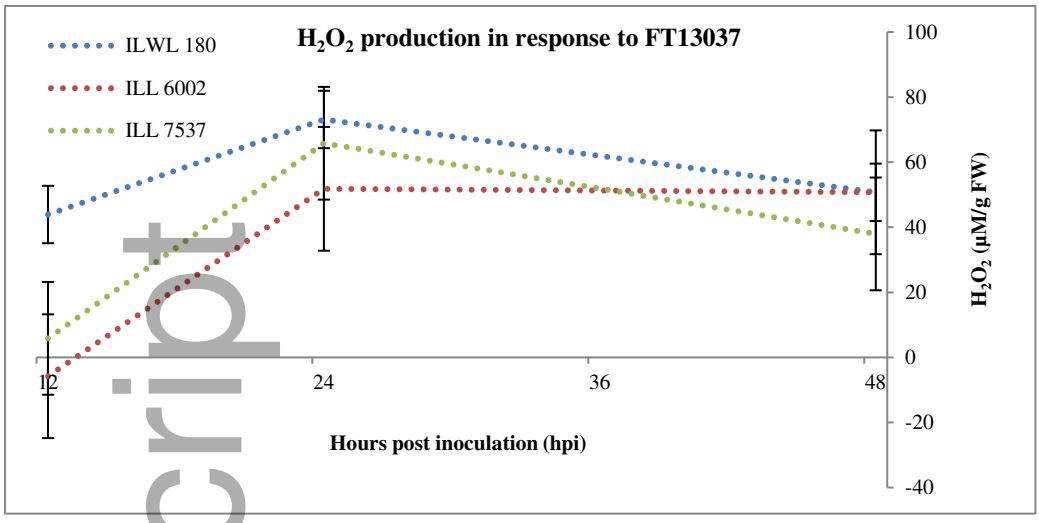

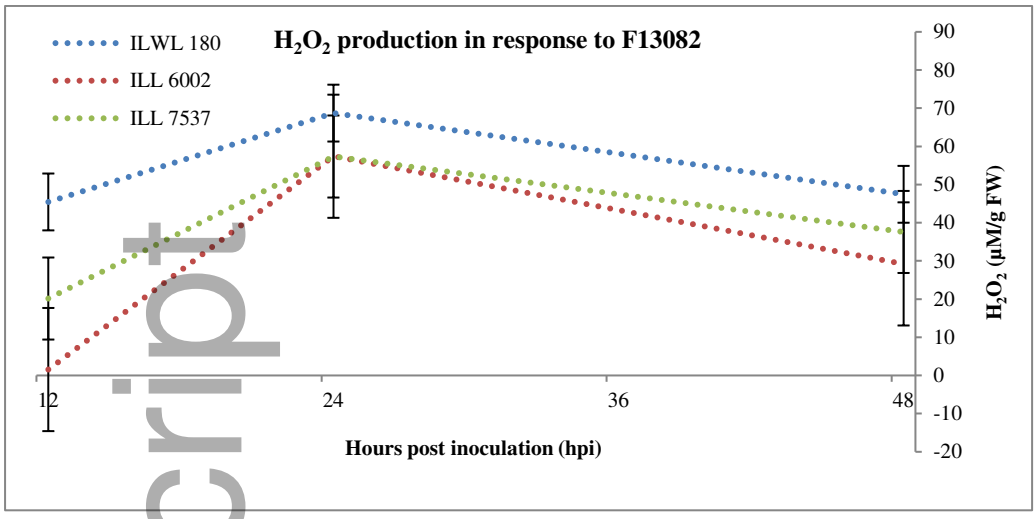

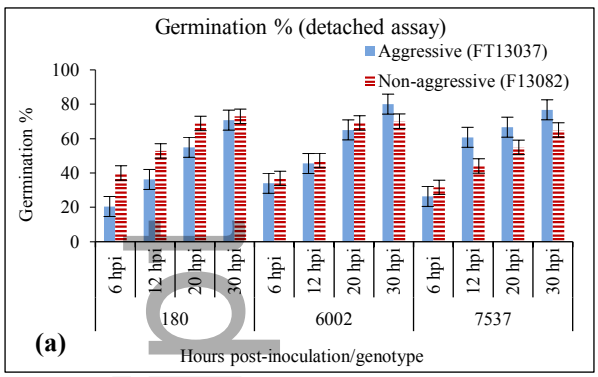

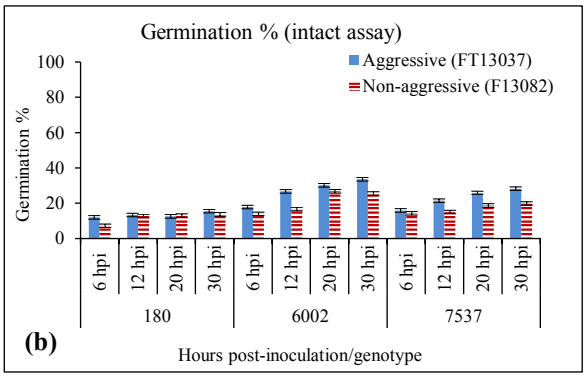

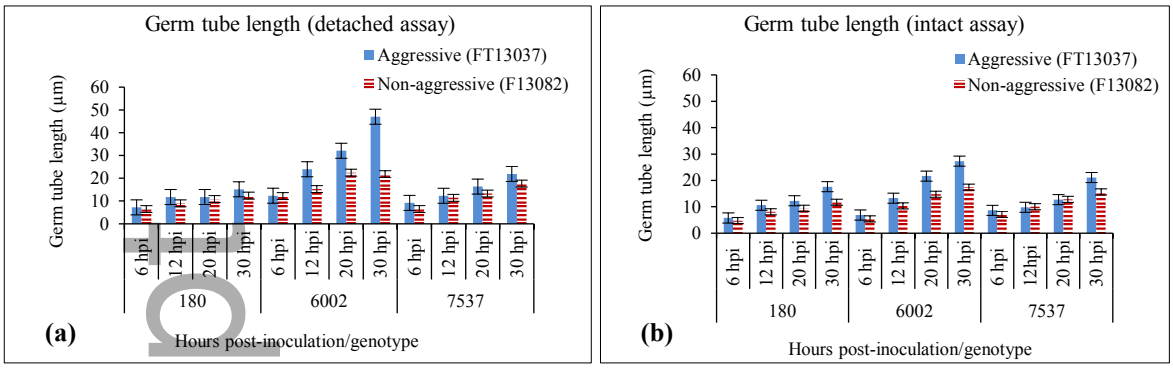

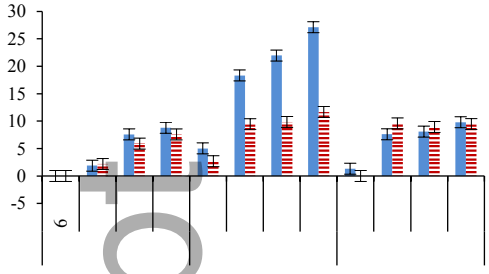

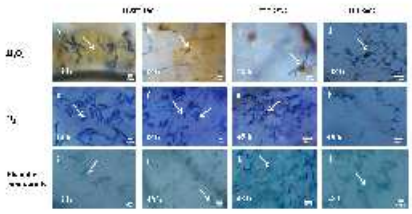

ppa_12851_f4.tif

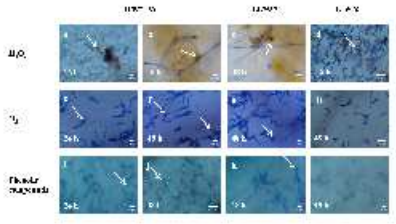

ppa_12851_f5.tif